

Dynamics of three coupled van der Pol oscillators with application to circadian rhythms

Kevin Rompala ^a, Richard Rand ^{a,*}, Howard Howland ^b

^a *Department of Theoretical and Applied Mechanics, Cornell University, Ithaca, NY 14853, USA*

^b *Department of Neurobiology and Behavior, Cornell University, Ithaca, NY 14853, USA*

Received 11 August 2005; received in revised form 11 August 2005; accepted 12 August 2005

Available online 21 September 2005

Abstract

In this work we study a system of three van der Pol oscillators. Two of the oscillators are identical, and are not directly coupled to each other, but rather are coupled via the third oscillator. We investigate the existence of the in-phase mode in which the two identical oscillators have the same behavior. To this end we use the two variable expansion perturbation method (also known as multiple scales) to obtain a slow flow, which we then analyze using the computer algebra system MACSYMA and the numerical bifurcation software AUTO.

Our motivation for studying this system comes from the presence of circadian rhythms in the chemistry of the eyes. We model the circadian oscillator in each eye as a van der Pol oscillator. Although there is no direct connection between the two eyes, they are both connected to the brain, especially to the pineal gland, which is here represented by a third van der Pol oscillator.

© 2005 Elsevier B.V. All rights reserved.

PACS: 02.30.Hq; 02.30.Mv; 02.30.Oz; 02.60.Cb

Keywords: Coupled oscillators; Phase-locking; Perturbation; Bifurcation

1. Introduction

In this work we study a system of three van der Pol oscillators, x , y and w , coupled as follows:

$$\ddot{x} - \epsilon(1 - x^2)\dot{x} + x = \epsilon\mu(w - x) \quad (1)$$

$$\ddot{y} - \epsilon(1 - y^2)\dot{y} + y = \epsilon\mu(w - y) \quad (2)$$

$$\ddot{w} - \epsilon(1 - w^2)\dot{w} + p^2w = \epsilon\mu(x - w) + \epsilon\mu(y - w) \quad (3)$$

Here the x and y oscillators are identical, and are not directly coupled to each other, but rather are coupled via the w oscillator.

* Corresponding author. Tel.: +1 607 255 7145; fax: +1 607 255 2011.

E-mail addresses: krr26@cornell.edu (K. Rompala), rrh2@cornell.edu (R. Rand), hch2@cornell.edu (H. Howland).

Our motivation for studying this system comes from the presence of circadian rhythms in the chemistry of the eyes. We model the circadian oscillator in each eye as a van der Pol oscillator (x and y). Although there is no direct connection between the two eyes, they are both connected to the brain, especially to the pineal gland, which is here represented by a third van der Pol oscillator (w).

Experiments on quail chicks have shown that when they are placed in constant light conditions (representing an autonomous system with no external forcing), the level of melatonin in their two eyes are found to be in-phase after a period of more than 40 days [4]. This in-phase stability seems to hold for a wide range of initial conditions, even, e.g., if the two eyes are initially light-loaded to be out of phase [4]. (This may be accomplished experimentally by placing an opaque patch on the left eye (but none on the right eye) for 12 h, then switching the opaque patch to the right eye for 12 h, and then repeating this for several days.)

In a previous attempt to explain this phenomenon, the system was modeled as two van der Pol oscillators coupled by a “bath” [6]

$$\ddot{x} - \epsilon(1 - x^2)\dot{x} + x = k(z - x) \tag{4}$$

$$\ddot{y} - \epsilon(1 - y^2)\dot{y} + y = k(z - y) \tag{5}$$

$$\dot{z} = k(x - z) + k(y - z) \tag{6}$$

The idea of this model is that the two eyes influence each other by affecting the concentration of a substance (melatonin) in the bloodstream. Here the non-oscillatory bath represents the bloodstream. Unfortunately this model predicted that the out-of-phase mode had greater stability than the in-phase mode, contrary to the experimental results.

Thus we were led to consider the system (1)–(3), which replaces the bath coupling z by coupling via the avian pineal gland in the brain, represented by the w oscillator. The avian pineal gland has been shown to secrete melatonin in an oscillatory fashion (with high levels during the night and low levels during daylight hours) and thus is also modeled as a van der Pol oscillator.

This model consisting of the eyes and the pineal gland of the chick constitutes only a subset of the entire avian circadian system (see [5] for review). Assumptions made are that the putative suprachiasmatic nucleus (SCN) of the chick and the pineal gland remain intact and that we are considering only free-running behavior (represented by the autonomous nature of the equations). We consider melatonin levels as a possible coupling scheme (either directly or through an un-modeled intermediary) between the eyes and pineal gland.

The question which we are most interested in answering is what are the stabilities of the in-phase and out-of-phase modes? The present paper does not answer this question, but rather considers just the question of the *existence* of the in-phase mode. The in-phase mode $x = y$ satisfies the equations:

$$\ddot{x} - \epsilon(1 - x^2)\dot{x} + x = \epsilon\mu(w - x) \tag{7}$$

$$\ddot{w} - \epsilon(1 - w^2)\dot{w} + p^2w = 2\epsilon\mu(x - w) \tag{8}$$

Eqs. (7) and (8) represent a four-dimensional invariant manifold which sits inside the six-dimensional phase space of Eqs. (1)–(3). In this paper we are interested in asking for which parameters a stable periodic motion exists in Eqs. (7) and (8). It should be noted that although a periodic motion is stable in the four-dimensional invariant manifold of Eqs. (7) and (8), it may not be stable in the larger six-dimensional space of Eqs. (1)–(3).

2. Perturbation expansion

We study the in-phase mode equations (7) and (8) for small values of ϵ . We use the two variable expansion method [2] and replace t by two new independent variables, $\xi = t$ and $\eta = \epsilon t$. Eqs. (7) and (8) become, neglecting terms of $O(\epsilon^2)$:

$$\frac{\partial^2 x}{\partial \xi^2} + 2\epsilon \frac{\partial^2 x}{\partial \xi \partial \eta} - \epsilon(1 - x^2) \frac{\partial x}{\partial \xi} + x = \epsilon\mu(w - x) \tag{9}$$

$$\frac{\partial^2 w}{\partial \xi^2} + 2\epsilon \frac{\partial^2 w}{\partial \xi \partial \eta} - \epsilon(1 - w^2) \frac{\partial w}{\partial \xi} + p^2w = 2\epsilon\mu(x - w) \tag{10}$$

Next we assume that the frequency p of the w oscillator is close to that of the x and y oscillators, and we expand

$$p = 1 + \epsilon \Delta \quad (11)$$

We expand both x and w in power series of ϵ

$$x = x_0(\xi, \eta) + \epsilon x_1(\xi, \eta), \quad w = w_0(\xi, \eta) + \epsilon w_1(\xi, \eta) \quad (12)$$

We substitute Eqs. (11) and (12) into (9) and (10) and collect terms, giving at $O(\epsilon^0)$

$$\frac{\partial^2 x_0}{\partial \xi^2} + x_0 = 0, \quad \frac{\partial^2 w_0}{\partial \xi^2} + w_0 = 0 \quad (13)$$

while at $O(\epsilon^1)$

$$\frac{\partial^2 x_1}{\partial \xi^2} + x_1 = -2 \frac{\partial^2 x_0}{\partial \xi \partial \eta} - (1 - x_0^2) \frac{\partial x_0}{\partial \xi} + \mu(w_0 - x_0) \quad (14)$$

$$\frac{\partial^2 w_1}{\partial \xi^2} + w_1 = -2 \frac{\partial^2 w_0}{\partial \xi \partial \eta} - (1 - w_0^2) \frac{\partial w_0}{\partial \xi} - 2\Delta w_0 + 2\mu(x_0 - w_0) \quad (15)$$

We take the solutions of Eqs. (13) in the form

$$x_0 = R_1(\eta) \cos(\xi - \theta_1(\eta)), \quad w_0 = R_2(\eta) \cos(\xi - \theta_2(\eta)) \quad (16)$$

where R_1 , R_2 , θ_1 and θ_2 are as yet undetermined functions of slow time η . Next we substitute (16) into (14) and (15) and eliminate secular terms. This gives the following slow flow:

$$\frac{dR_1}{d\eta} = \frac{R_1}{2} - \frac{R_1^3}{8} - \mu \frac{R_2}{2} \sin \phi \quad (17)$$

$$\frac{dR_2}{d\eta} = \frac{R_2}{2} - \frac{R_2^3}{8} + \mu R_1 \sin \phi \quad (18)$$

$$\frac{d\theta_1}{d\eta} = -\frac{\mu}{2} + \frac{\mu}{2} \frac{R_2}{R_1} \cos \phi \quad (19)$$

$$\frac{d\theta_2}{d\eta} = -\Delta - \mu + \mu \frac{R_1}{R_2} \cos \phi \quad (20)$$

where we have set $\phi = \theta_2 - \theta_1$. Subtracting (19) from (20), we obtain

$$\frac{d\phi}{d\eta} = -\Delta - \frac{\mu}{2} + \frac{\mu}{2} \left(2 \frac{R_1}{R_2} - \frac{R_2}{R_1} \right) \cos \phi \quad (21)$$

The three slow-flow equations (17), (18) and (21) are defined on a phase space with topology $R^+ \times R^+ \times S^1$. An equilibrium point in this slow flow corresponds to a periodic motion of the system (7) and (8), that is, to an in-phase mode of the 3-oscillator system (1)–(3).

3. Bifurcation analysis

Using the computer algebra system MACSYMA, we manipulate the RHS's of Eqs. (17), (18) and (21) to compute conditions on the parameters μ and Δ for saddle-node and Hopf bifurcations. The details of this complicated calculation are given in Appendix A. The results are plotted in Fig. 1. The condition (24) for saddle-node bifurcations plots as two triangular-shaped curves in Fig. 1 and corresponds to a pair of slow-flow equilibria merging together. The condition (27) for Hopf bifurcations plots as two parabola-shaped curves in Fig. 1 and corresponds to an equilibrium point of the focus (or spiral) type which changes stability, giving birth to a limit cycle. The portions of the Hopf curves which lie inside the triangular regions (shown dashed in Fig. 1) do not represent a bifurcation, as explained at the end of Appendix A.

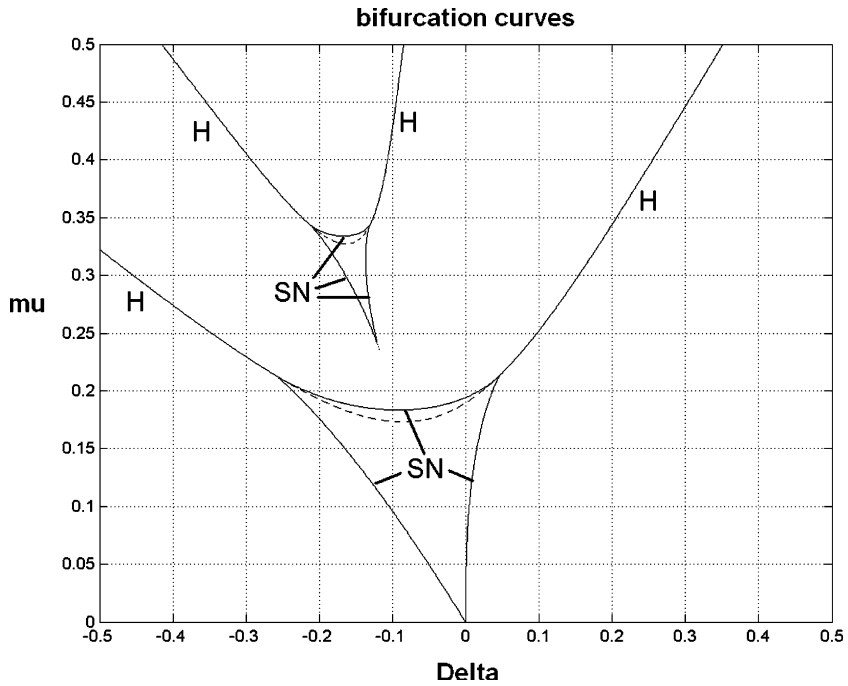


Fig. 1. Bifurcation curves of the slow-flow (17), (18) and (21) obtained in closed form by use of the computer algebra system MACSYMA, see Appendix A. The two triangular-shaped curves are given by Eq. (24) and represent saddle-node bifurcations (SN). The two parabola-shaped curves are given by Eq. (27) and represent Hopf bifurcations (H).

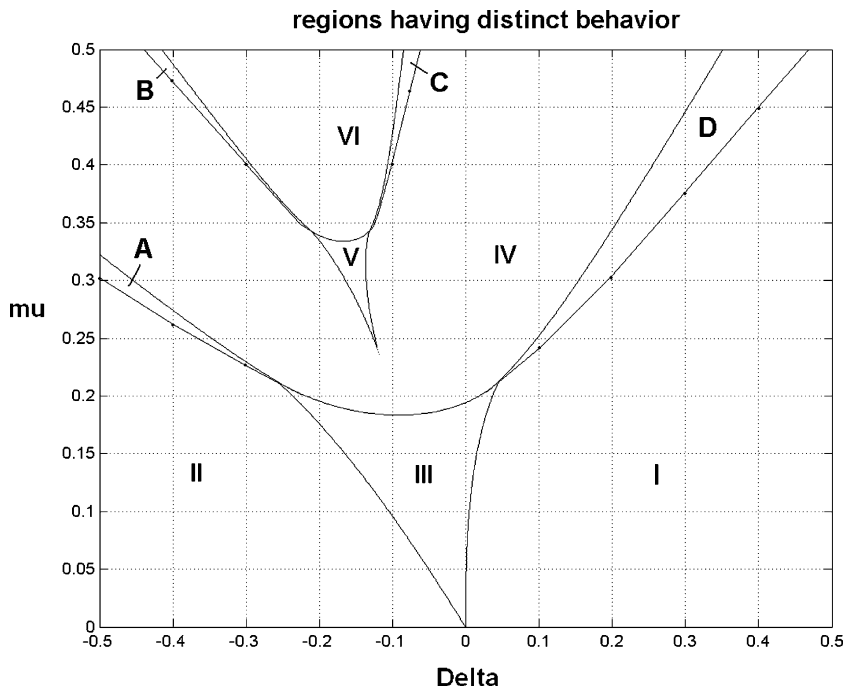


Fig. 2. The bifurcation curves in Fig. 1 are supplemented by four additional bifurcation curves which were obtained numerically, resulting in 10 regions in the parameter space, each having distinct dynamical features and behavior. See text.

The bifurcation curves in Fig. 1 are shown in Fig. 2, along with four additional bifurcation curves which were obtained numerically, resulting in 10 regions in the parameter space, each having distinct dynamical features and behavior.

Numerical integration of the slow-flow equations reveals three primary types of behavior in our original in-phase subspace: (i) phase-drift (positive and negative), (ii) weakly phase-locked motions, and (iii) phase-locked motions. See Fig. 3.

(i) Phase-drift occurs when the phase-difference $\phi(\eta)$ between the pineal (w) oscillator and the eye ($x = y$) oscillators increases (or decreases) without bound. In the $R^+ \times R^+ \times S^1$ phase space, phase-drift appears as a closed curve (a limit cycle) which is cyclic in ϕ . Positive (negative) drift refers to the direction of the flow in ϕ . We will refer to such a motion as an

LCD(= limit cycle with drift)

(ii) A weakly phase-locked motion occurs when $\phi(\eta)$ is periodic. It is represented in the phase space by a limit cycle which is topologically distinct from the drift limit cycle. In this system, such weakly phase-locked limit cycles are born in a Hopf bifurcation, that is, they start out as very small topological circles. We will refer to such a motion as an

LCW(= limit cycle with weak phase-locking)

(iii) Phase-locked motions are motions where $\phi(\eta)$ remains constant. These motions correspond to equilibria in the slow-flow phase space.

The particular features found in each region of Fig. 2 are described as follows:

REGION I: There exist two unstable equilibrium points and a stable LCD. All trajectories in the phase space experience negative drift.

REGION II: There exist two unstable equilibrium points and a stable LCD. All trajectories in the phase space experience positive drift.

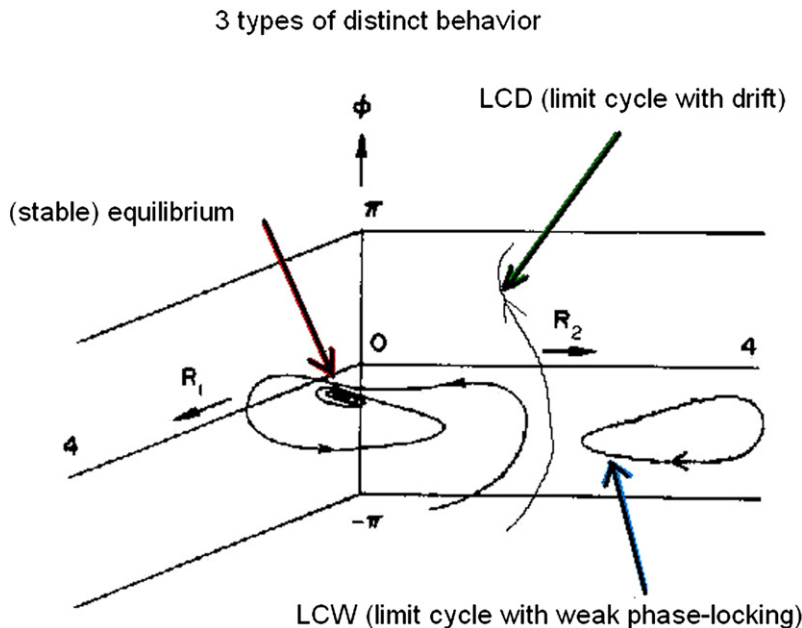


Fig. 3. Schematic diagram showing the three primary types of behavior found in the slow-flow equations (17), (18) and (21): (i) LCD = limit cycle with drift, (ii) LCW = limit cycle with weak phase-locking, and (iii) phase-locked motions (slow-flow equilibria). Note that the LCD is a closed curve because of the $R^+ \times R^+ \times S^1$ topology of the phase space, i.e., the upper boundary $\phi = \pi$ is identified with the lower boundary $\phi = -\pi$.

REGION III: There exist one stable and three unstable equilibrium points. All trajectories tend to the stable equilibrium point.

REGION IV: There exist one stable and one unstable equilibrium point. All trajectories tend to the stable equilibrium point.

REGION V: There exist two stable and two unstable equilibrium points. All trajectories are attracted to one of the two stable equilibrium points.

REGION VI: There exist two stable equilibrium points. All trajectories are attracted to one of the two stable equilibrium points. There also exists an unstable LCD.

REGIONS A and D: There exist two unstable equilibrium points and a stable LCW. All trajectories approach the stable limit cycle.

REGIONS B and C: There exist one stable and one unstable equilibrium point and a stable LCW. All trajectories are attracted to either the stable equilibrium point or to the stable LCW. In addition there exists an unstable motion which is an LCD at the region VI side of regions B, C, but which is an LCW at the region IV side of regions B, C. The change from LCD to LCW occurs along a curve (unmarked in Fig. 2) in each of regions B, C via a saddle-connection bifurcation [3].

Of particular interest are the bifurcations occurring on the lower boundaries of regions A and D. These involve the conversion of stable LCW's to stable LCD's via collisions with the singular surfaces $R_1 = 0$ or $R_2 = 0$ and the formation of saddle-connections [1]. Starting in region IV, we have one stable and one unstable equilibrium point. Crossing from region IV to region D, a supercritical Hopf bifurcation occurs and a stable LCW (weakly phase-locked motion) appears. As we continue traveling further into region D the limit cycle increases in size until it collides with a singular surface and forms a saddle-connection. The LCW then changes its topology to that of LCD (phase-drift). This bifurcation occurs on the lower boundary of region D. The same scenario occurs in region A.

The LCD which is born out of an LCW on the lower boundary of region D continues to exist throughout region I. However, it is destroyed in an infinite period bifurcation as we cross from region I to region III. This

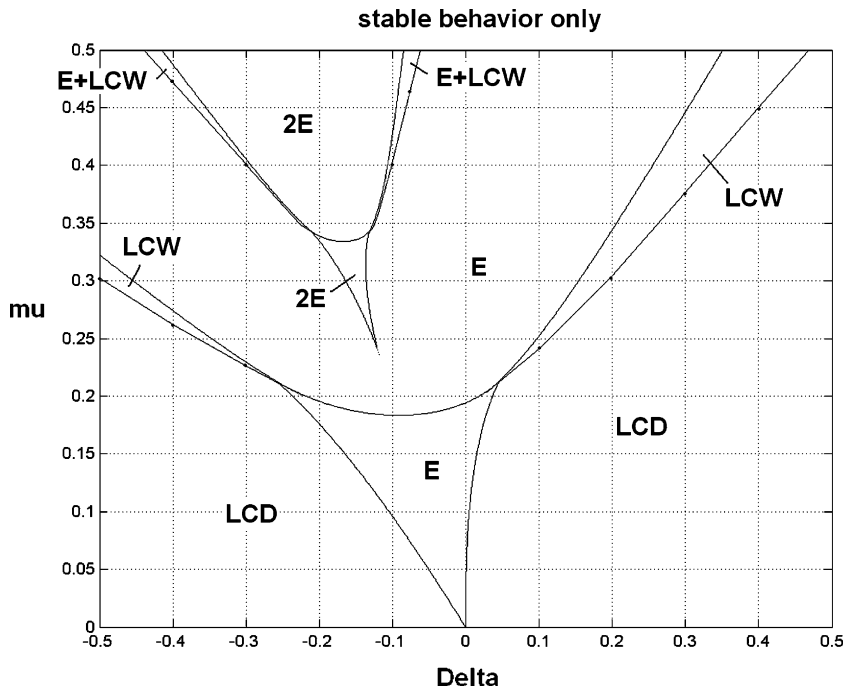


Fig. 4. The 10 regions of Fig. 2 shown with their stable behavior (unstable motions not shown). E = slow-flow equilibrium, 2E = two stable equilibria, LCD = limit cycle with drift, LCW = limit cycle with weak phase-locking.

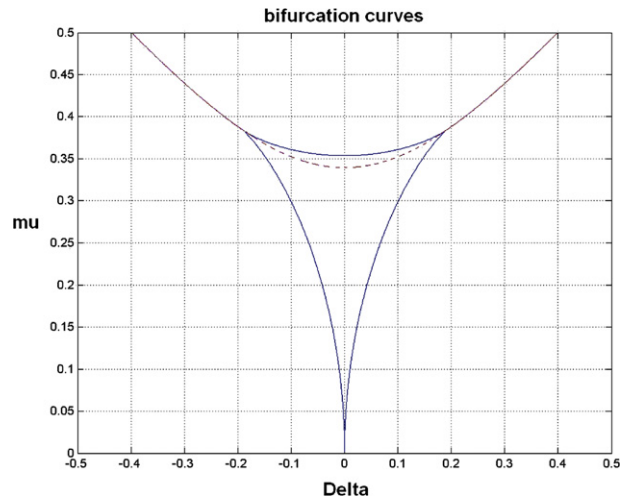


Fig. 5. Bifurcation curves for a system of two directly coupled van der Pol oscillators [2], Eqs. (22) and (23). Compare with Fig. 1.

infinite period bifurcation is, in addition, a saddle-node bifurcation, which increases the number of slow-flow equilibria from two in region I to four in region III. The same scenario occurs in regions A–II–III.

A supercritical Hopf bifurcation occurs and a stable LCW is born as we cross the boundary between regions VI and C. This LCW is destroyed as we move into region IV, where it coalesces with an unstable LCW. The same scenario occurs in regions VI–B–IV.

In Fig. 4 we show the stable behavior in each of the regions of parameter space of Fig. 2.

4. Conclusions

In this paper we have investigated the existence of the in-phase mode in a particular system of three weakly coupled van der Pol oscillators, Eqs. (1)–(3). Although the setting for original problem is a six-dimensional phase space, the in-phase mode lives in a four-dimensional invariant subspace given by Eqs. (7) and (8). Using the two-variable expansion perturbation method, we reduced the four-dimensional in-phase subspace to a three-dimensional slow flow given by Eqs. (17), (18) and (21). Using computational tools (AUTO, MACSYMA, MATLAB) we were able to successfully compute (both numerically and analytically) the bifurcation curves for the slow flow. The qualitative behavior in the slow flow and in the four-dimensional in-phase subspace was determined for each distinct region in the parameter plane of Fig. 2.

It is interesting to compare the dynamics of the in-phase mode in the present problem with the dynamics of two directly coupled van der Pol oscillators [2]

$$\ddot{x} - \epsilon(1 - x^2)\dot{x} + x = \epsilon\mu(w - x) \quad (22)$$

$$\ddot{w} - \epsilon(1 - w^2)\dot{w} + p^2w = \epsilon\mu(x - w) \quad (23)$$

Comparison of Eqs. (22) and (23) with Eqs. (7) and (8) reveals the presence of an extra factor of 2 on the RHS of Eq. (8) compared with the RHS of Eq. (23). Fig. 5 [2] shows the bifurcation curves for Eqs. (22) and (23) comparable to Fig. 1. Various types of dynamical behavior found in Eqs. (22) and (23) also occur in Eqs. (7) and (8), including stable and unstable phase-locked motion, weakly phase-locked motion, and drift. However, as Figs. 1, 2 and 5 show, Eqs. (7) and (8) involve four new regions of the parameter plane which do not occur in Eqs. (22) and (23), namely regions V, VI, B and C. All of these four regions contain multiple steady states. Regions V and VI contain two stable phase-locked motions while regions B and C contain one stable phase-locked motion and one stable weakly phase-locked motion.

In the context of our biological application, the in-phase motion investigated in this paper corresponds to the synchronized periodic behavior of circadian rhythms in each of the two eyes (modeled by x and y oscillators), as well as in the brain (modeled by the w oscillator). Of biological importance is the existence of stable equilibria in the slow flow (all regions except I and II). These correspond to stable phase-locked in-phase mo-

tions of the original four-dimensional in-phase problem. The biological phenomenon associated with the four regions which exhibit multiple steady states will include dependence of the steady state on initial conditions and associated hysteresis. Note that this interesting dynamical behavior occurs when $\Delta < 0$ (assuming $\mu > 0$). This corresponds to the situation where the eye oscillators have a higher frequency (and thus shorter period) than the brain oscillator.

It is important to realize that we have not yet studied the stability of the in-phase subspace. Thus although a slow-flow equilibrium (and associated periodic motion of Eqs. (7) and (8)) may be stable with respect to the in-phase subspace, it may turn out to be unstable with respect to the original six-dimensional phase space of Eqs. (1)–(3). We plan to investigate the stability of such motions in the original six-dimensional phase space in future work.

Acknowledgement

Portions of this work were supported by NIH NEI grant 02994 to HCH.

Appendix A

The following scheme by which we determine conditions for saddle-node and Hopf bifurcations of slow-flow equilibria is based on the treatment of two coupled van der Pol oscillators in Chapter 9 of [2]. This calculation is algebraically complicated and was done using the computer algebra system MACSYMA. We begin by algebraically eliminating R_2 and ϕ from the three equilibrium equations represented by the vanishing of RHS's of (17), (18) and (21), thereby leaving an equation which depends on R_1 only. We multiply (17) by $2R_1$ and (18) by R_2 , and add them together. This yields an algebraic equation which involves R_1 and R_2 , but not ϕ . Let us refer to it as Eq. (A). Next we multiply (17) by R_2 and (18) by R_1 , and subtract them. We solve the resulting equation for $\sin \phi$ and refer to the result as Eq. (B). Next we solve (21) for $\cos \phi$ and refer to the result as Eq. (C). Then we combine Eqs. (B) and (C) using the identity $\sin^2 \phi + \cos^2 \phi = 1$ and obtain an equation which involves R_1 and R_2 , but not ϕ . We refer to it as Eq. (D). Next we algebraically eliminate R_2 from Eqs. (A) and (D), yielding an equation on R_1 only (no ϕ or R_2). We refer to it as Eq. (E). Now for a saddle-node bifurcation, Eq. (E) must have a double root. Thus we differentiate Eq. (E) with respect to R_2 , obtaining an equation which we refer to as Eq. (F). Then we eliminate R_2 between Eqs. (E) and (F), which gives the condition for a saddle-node as Eq. (24). This equation plots as triangle-shaped curves in Fig. 1:

$$\begin{aligned}
 &45349632\mu^{14} + 221709312\Delta\mu^{13} + 690508800\Delta^2\mu^{12} + 9027936\mu^{12} \\
 &+ 1492475904\Delta^3\mu^{11} + 38320128\Delta\mu^{11} + 2529857536\Delta^4\mu^{10} + 105827328\Delta^2\mu^{10} \\
 &- 4323051\mu^{10} + 3420995584\Delta^5\mu^9 + 231647232\Delta^3\mu^9 - 15105708\Delta\mu^9 \\
 &+ 3827613696\Delta^6\mu^8 + 453522432\Delta^4\mu^8 - 35909484\Delta^2\mu^8 + 539217\mu^8 \\
 &+ 3541827584\Delta^7\mu^7 + 721944576\Delta^5\mu^7 - 63304320\Delta^3\mu^7 + 3036832\Delta\mu^7 \\
 &+ 2745761792\Delta^8\mu^6 + 919879680\Delta^6\mu^6 - 80637888\Delta^4\mu^6 + 8802064\Delta^2\mu^6 \\
 &- 12636\mu^6 + 1759248384\Delta^9\mu^5 + 912162816\Delta^7\mu^5 - 38032128\Delta^5\mu^5 \\
 &+ 7835616\Delta^3\mu^5 - 183192\Delta\mu^5 + 930873344\Delta^{10}\mu^4 + 701669376\Delta^8\mu^4 \\
 &+ 40007424\Delta^6\mu^4 - 3381904\Delta^4\mu^4 - 841176\Delta^2\mu^4 - 81\mu^4 + 392167424\Delta^{11}\mu^3 \\
 &+ 410910720\Delta^9\mu^3 + 81358848\Delta^7\mu^3 - 3334912\Delta^5\mu^3 - 1019520\Delta^3\mu^3 \\
 &+ 2640\Delta\mu^3 + 128974848\Delta^{12}\mu^2 + 177340416\Delta^{10}\mu^2 + 65590272\Delta^8\mu^2 \\
 &+ 7929600\Delta^6\mu^2 + 231360\Delta^4\mu^2 + 20304\Delta^2\mu^2 + 29360128\Delta^{13}\mu + 51904512\Delta^{11}\mu \\
 &+ 30167040\Delta^9\mu + 7749632\Delta^7\mu + 889344\Delta^5\mu + 35328\Delta^3\mu + 16\Delta\mu + 4194304\Delta^{14} \\
 &+ 8650752\Delta^{12} + 6033408\Delta^{10} + 1937408\Delta^8 + 296448\Delta^6 + 17664\Delta^4 + 16\Delta^2 = 0
 \end{aligned}
 \tag{24}$$

To find a comparable condition for a Hopf bifurcation, we compute the 3×3 Jacobian matrix based on Eqs. (17), (18) and (21) and use Eqs. (B) and (C) to eliminate ϕ from the matrix elements. Then we compute the characteristic polynomial of this matrix, which is of the form:

$$\lambda^3 + c_2\lambda^2 + c_1\lambda + c_0 = 0 \quad (25)$$

For a Hopf bifurcation, we require λ to be pure imaginary. Thus the eigenvalues λ will include a pure imaginary pair, $\pm i\beta$, and a real eigenvalue, γ . This requires the characteristic polynomial to have the form:

$$\lambda^3 - \gamma\lambda^2 + \beta^2\lambda - \beta^2\gamma = 0 \quad (26)$$

Comparing Eqs. (25) and (26), we see that a necessary condition for a Hopf is

$$c_0 = c_1c_2$$

Let us call this Eq. (G). Next we use Eq. (A) to eliminate R_2 from Eq. (G). The resulting equation contains R_1 only (no ϕ or R_2). We refer to it as Eq. (H). Finally we use Eq. (E) to eliminate R_1 from Eq. (H), which gives the following condition (27) for a Hopf bifurcation:

$$\begin{aligned} &206046997776\mu^{16} + 128246239872\Delta\mu^{15} - 1055299653504\Delta^2\mu^{14} + 151716144096\mu^{14} \\ &- 4792910330880\Delta^3\mu^{13} - 959470912224\Delta\mu^{13} - 10067384941056\Delta^4\mu^{12} - 4022175416544\Delta^2\mu^{12} \\ &- 76183604811\mu^{12} - 13620666378240\Delta^5\mu^{11} - 8422624949760\Delta^3\mu^{11} - 1162076374872\Delta\mu^{11} \\ &- 11038023456768\Delta^6\mu^{10} - 9771098692608\Delta^4\mu^{10} - 2453769115848\Delta^2\mu^{10} - 53727633963\mu^{10} \\ &- 1633265565696\Delta^7\mu^9 - 5111334563328\Delta^5\mu^9 - 2698414682336\Delta^3\mu^9 - 368730619308\Delta\mu^9 \\ &+ 10450239639552\Delta^8\mu^8 + 4596633773568\Delta^6\mu^8 - 930295796592\Delta^4\mu^8 - 500042378940\Delta^2\mu^8 \\ &- 10567871928\mu^8 + 18955313086464\Delta^9\mu^7 + 14654584700928\Delta^7\mu^7 + 2928072365568\Delta^5\mu^7 \\ &- 65251243872\Delta^3\mu^7 - 43666800936\Delta\mu^7 + 20325924864000\Delta^{10}\mu^6 + 19734795325440\Delta^8\mu^6 \\ &+ 6459457683968\Delta^6\mu^6 + 646749530928\Delta^4\mu^6 - 25863482760\Delta^2\mu^6 - 842897393\mu^6 \\ &+ 15864307384320\Delta^{11}\mu^5 + 18526299439104\Delta^9\mu^5 + 7894980157440\Delta^7\mu^5 + 1385895931968\Delta^5\mu^5 \\ &+ 75604570176\Delta^3\mu^5 - 1221626868\Delta\mu^5 + 9417278619648\Delta^{12}\mu^4 + 12970012852224\Delta^{10}\mu^4 \\ &+ 6670762715136\Delta^8\mu^4 + 1563045302976\Delta^6\mu^4 + 151762831008\Delta^4\mu^4 + 2639537484\Delta^2\mu^4 \\ &- 16895076\mu^4 + 4277139406848\Delta^{13}\mu^3 + 6902205382656\Delta^{11}\mu^3 + 4225522688000\Delta^9\mu^3 \\ &+ 1243790340096\Delta^7\mu^3 + 175856646912\Delta^5\mu^3 + 9882465920\Delta^3\mu^3 + 104063568\Delta\mu^3 \\ &+ 1433187385344\Delta^{14}\mu^2 + 2690954035200\Delta^{12}\mu^2 + 1939282108416\Delta^{10}\mu^2 + 685956946944\Delta^8\mu^2 \\ &+ 123792201984\Delta^6\mu^2 + 10341576000\Delta^4\mu^2 + 273469584\Delta^2\mu^2 + 1086528\mu^2 + 328866988032\Delta^{15}\mu \\ &+ 711039909888\Delta^{13}\mu + 596824129536\Delta^{11}\mu + 250006241280\Delta^9\mu + 55862845440\Delta^7\mu \\ &+ 6480411648\Delta^5\mu + 338812032\Delta^3\mu + 5262144\Delta\mu + 41108373504\Delta^{16} + 101577129984\Delta^{14} \\ &+ 99470688256\Delta^{12} + 50001248256\Delta^{10} + 13965711360\Delta^8 + 2160137216\Delta^6 \\ &+ 169406016\Delta^4 + 5262144\Delta^2 + 43264 = 0 \end{aligned} \quad (27)$$

Note that when Eq. (27) is plotted in Fig. 1, the portion of each of the two branches which lies inside the triangular regions is shown dashed. In these regions the quantity β^2 referred to in Eq. (26) is negative so that the eigenvalue $\lambda = \pm i\beta$ is not imaginary, and no Hopf occurs there.

References

- [1] Chakraborty T, Rand RH. The transition from phase locking to drift in a system of two weakly coupled van der Pol oscillators. *Int J Nonlinear Mech* 1988;23:369–76.
- [2] Rand RH. *Lecture notes in nonlinear vibrations* (version 45). Ithaca, NY: The Internet-First University Press; 2004. Available from: <http://dSPACE.library.cornell.edu/handle/1813/79>.

- [3] Rompala K. MS thesis, Cornell University, 2005.
- [4] Steele CT, Zivkovic BD, Siopes T, Underwood H. Ocular clocks are tightly coupled and act as pacemakers in the circadian system of Japanese quail. *Am J Physiol Regul Integrat Comp Physiol* 2003;284:R208–18.
- [5] Underwood H, Steele CT, Zivkovic B. Circadian organization and the role of the pineal in birds. *Microscopy Res Tech* 2001;53:48–62.
- [6] Wirkus E, Rand R, Howland H. Dynamics of two van der Pol oscillators coupled via a bath. *Int J Solids Struct* 2004;41:2133–43.